Analytically Solvable Model of Photonic Crystal Structures and Novel Phenomena

Shojiro Kawakami, *Life Fellow, IEEE*

***Abstract*—The purpose of this work is twofold. First, we present a new simple model of photonic crystal structures that can be treated analytically. Second, from the rigorous analysis of propagation and resonance of the models, we point out two novel properties of waves in the structure. The first is that there is a waveguide in which a leakage-free guided mode can have the same propagation constant (wavenumber) as that of continuum waves. The second novel property is that there is a resonator in which the wave can be localized, even in the absence of a "full bandgap." These facts disprove some "common beliefs" about photonic crystal structures: many people believe that 1) in a photonic crystal waveguide, a radiation-free guided mode *cannot* have the same wavenumber as that of continuum modes and 2) in a photonic crystal resonator, lossless localization can take place *only if* the host photonic crystal has an absolute bandgap. Our examples show that such beliefs are overstatements.**

***Index Terms*—Analytic solution, circuit model, optical confinement, photonic crystal, propagation, resonator, waveguide.**

I. Introduction

PHOTONIC CRYSTALS gather much attention today because they have many fascinating properties, such as light localization [1] or the ability to guide light even along a sharp bend [2]. In this technical field, there are some fundamental points that many people take for granted but are not rigorously proved. This is due to the following two reasons. First, this new field has grown up very rapidly. Second, because it is difficult to analyze electromagnetic waves in photonic crystals, one usually has no other choice than to use computers to derive quantitative results. For example, the structures shown in Fig. 1 are frequently used as examples of photonic crystals, photonic crystal waveguides, and photonic crystal resonators. The propagation effects and resonances have been analyzed only numerically.

Our understandings of these systems consist of qualitative (or empirical in some sense) predictions combined with numerical results obtained by simulations. For example, as far as the structures of Fig. 1(c) and (d) are concerned, people apparently believe that, to realize a lossless ($Q = \infty$) resonator with a localized mode using a photonic crystal, a full-bandgap property [1] is a *must*. Likewise, it seems to be widely accepted that, in a line-defect photonic crystal waveguide, a guided mode turns leaky if it has the same longitudinal wavenumber as that of the continuum modes. (This is not mean to say that pioneers in this field [1], [2] stated these "common beliefs." Readers and followers seem to "extrapolate" earlier findings of pioneers.)

Manuscript received February 05, 2002; revised April 22, 2002.

The author is with the New Industry Creation Hatchery Center (NICHe), Tohoku University/Photonic Lattice, Inc., Sendai 980-8579, Japan (e-mail: kawakami@niche.tohoku.ac.jp).

Digital Object Identifier 10.1109/JLT.2002.800267

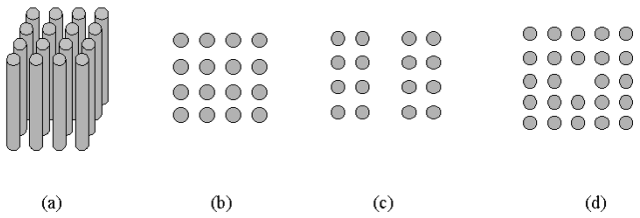

Fig. 1. Structures of 2-D photonic crystal structures. (a) Perspective. (b) Its top view. (c) A line-defect waveguide. (d) A point-defect resonator.

This paper presents a new simple model of two–dimensional (2-D) photonic crystal and its related structures (with defects) that can be solved analytically. The model provides rigorous proof against the above "common beliefs" about photonic crystal waveguides and resonators, i.e., we can state that 1) there is a situation in which a leakage-free guided mode has the same longitudinal wavenumber (propagation constant) as that of continuum waves and 2) a wave can be localized without loss even in the absence of a "full bandgap" within a region of the size comparable to a wavelength in the 2-D plane.

II. Analytically Solvable Structures

We assume a 2-D system uniform in the z direction and that the electric field is parallel to the z axis and the wave propagates in the xy plane (hence, the TE wave). Fig. 2(a), a perspective, represents an example of such a structure. Suppose it is seen from above [Fig. 2(b)]. For simplicity, we represent each structure by the top view. The structure in Fig. 2(c) represents an example of a line-defect waveguide, and the structure in Fig. 2(d) represents a resonator with crossed line defects. The wave equation for such 2-D systems is

$$\nabla^2\phi(x,y) + \omega^2\varepsilon(x,y)\mu_0\phi(x,y) = 0 \tag{1}$$

where ϕ stands for E_z. When the permittivity function is periodic with respect to x and y, analytic treatment of (1) is usually difficult.

Shepherd and Roberts [3] and other authors [4] circumvented the mathematical difficulty assuming that the function is a sum of delta functions. (Delta functions mean infinitely thin dielectric sheets with an infinite epsilon. The dielectric contrast is infinite and therefore physically unrealizable. Therefore, their model serves as an asymptotic model.)

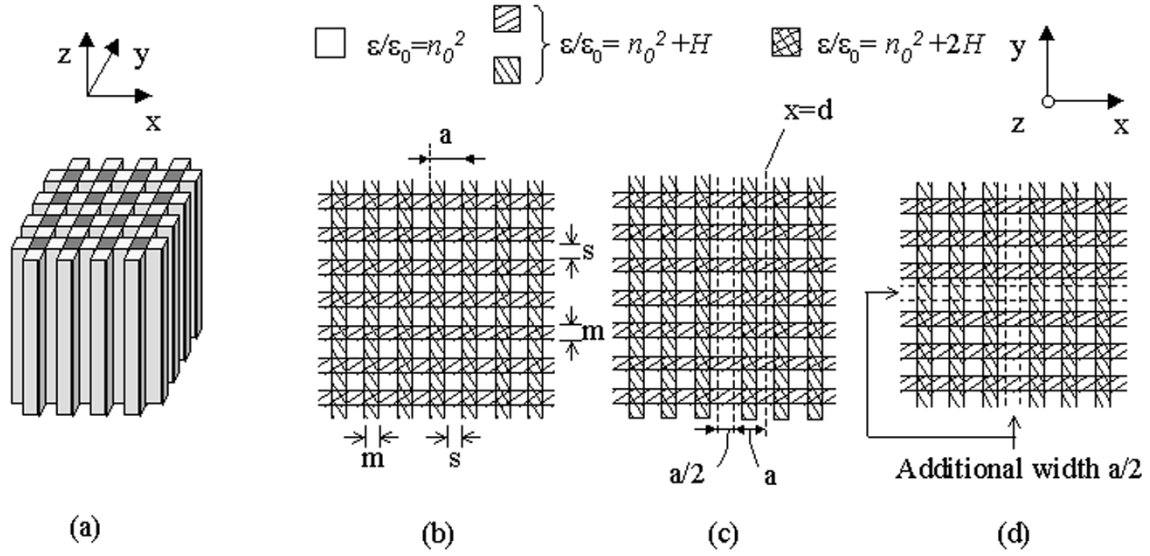

Fig. 2. Structures to be considered. (a) Perspective. (b) Top view. (c) A line-defect waveguide. (d) A crossed line-defect resonator.

We propose a new realizable alternative to it in which the dielectric contrast is finite. The point of our model is to assume

$$\varepsilon(x,y) = \varepsilon_0 \left(n_0^2 + f(x) + g(y)\right) \tag{2}$$

for which the wave (1) becomes separable. Assume $\phi = X(x)Y(y)$, and we obtain

$$X'' + k^2 \left(\frac{n_0^2}{2} + f(x) + K\right) X = 0$$

and

$$Y'' + k^2 \left(\frac{n_0^2}{2} + g(y) - K\right) Y = 0 \tag{3}$$

where k is the free space wavenumber ($k = 2\pi/\lambda$), and K is a constant of separation. There are many types of $f(x)$ and $g(y)$ that allow analytic treatment. The structures in Fig. 2(b) are typical. For the structure of Fig. 2(b), we consider

$$X'' + k^2\left(\nu^2 + f(x)\right)X = 0 \tag{4}$$

where $v^2 = n_0^2/2 + K$, $f(x)$ is shown in Fig. 3, and $f(x)$ and $g(y)$ are identical. The structures of Fig. 2(b), (c), and (d) all belong to the family of the analytically solvable and physically realizable structures. The permittivity function $\varepsilon(x,y)$ can be represented as $\varepsilon_0\left(n_0^2 + f(x) + g(y)\right)$; hence, the scalar wave equation becomes separable. The structures of Fig. 2(b), (c), and (d) are analyzed in Section III.

III. Analysis of Perfect Crystal, Line-Defect Waveguide, and a Resonator

In this section, we explain analytical approaches and present dispersion/resonance characteristics.

A. Perfectly Periodic Photonic Crystals

We consider a photonic crystal shown in Fig. 2(b). It has a square unit cell. The wave equations are given by (3), where $f(x) = g(y)$ and $f(x)$ is shown in Fig. 3. The differential equation can be treated by an electrical circuit analog [5], [6]: for each value of K (the separation constant), the circuit analog (Fig. 4) gives an eigen phase shift for the eigen excitation between 11 and $1'1'$, which is identical to $\beta_x a$, where β_x is the propagation constant (= wavenumber) in the x direction of the photonic crystal. Similarly, β_y (in the y direction) is obtained from the circuit analog corresponding to $-K$. For simplicity, we assume $m = s = a/2$ and focus only on the x part in the following. One half of the eigen phase shift multiplied by j is the same as the "image transfer constant" of the smallest unit 11–22 in Fig. 4(b). We will use the method of image parameters [5], which is ideally suited for closed-form analysis of periodic circuits. The method of an electrical model is very effective for two reasons.

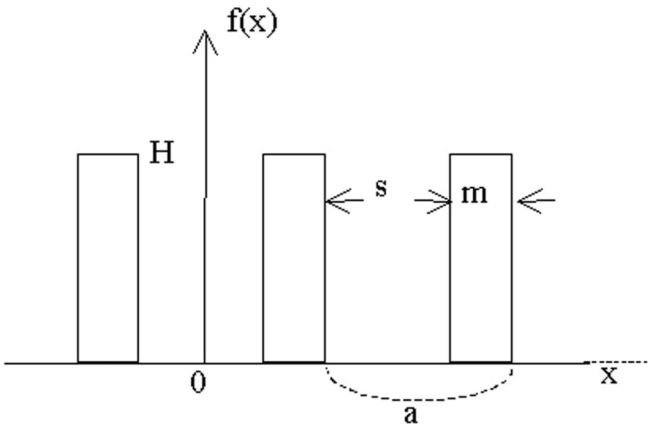

Fig. 3. Periodic rectangular potential function.

1) The electrical model changes a differential equation system into a simple matrix algebra.
2) The image impedance and the image transfer constant directly give the eigenvector and the eigenvalue of the system.

With the knowledge of image parameter analysis, we could write down equations almost automatically. For the reader's

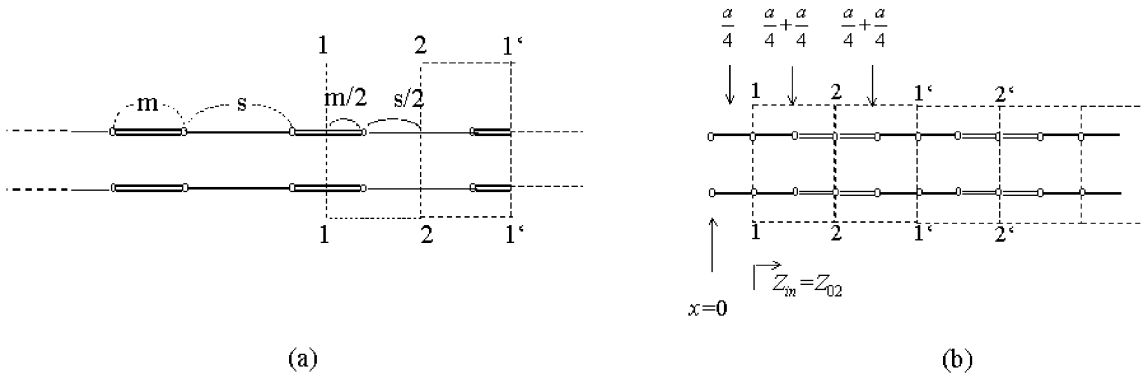

Fig. 4. (a) Cascaded transmission line analog representation of (3) with Fig. 3, where $W_m = W_0/(\nu^2 + H + K)^{1/2}$, $W_s = W_0/(\nu^2 + K)^{1/2}$, $\beta_m = k(\nu^2 + H + K)^{1/2}$, $\beta s = k(\nu^2 + K)^{1/2}$, and $W_0 = 120\pi$. (b) Transverse resonance model of the line-defect waveguide.

convenience, some important formulas are summarized in the Appendix. The transfer matrix of the section 11–22 is given by

$$\begin{bmatrix} A & B \\ C & D \end{bmatrix} = \begin{bmatrix} \cos\beta_m \frac{m}{2} & jW_m \sin\beta_m \frac{m}{2} \\ \frac{j\sin\beta_m \frac{m}{2}}{W_m} & \cos\beta_m \frac{m}{2} \end{bmatrix} \cdot \begin{bmatrix} \cos\beta_s \frac{s}{2} & jW_s \sin\beta_s \frac{s}{2} \\ \frac{j\sin\beta_s \frac{s}{2}}{W_s} & \cos\beta_s \frac{s}{2} \end{bmatrix} \tag{5}$$

$$\begin{bmatrix} V_1 \\ V_2 \end{bmatrix} = \begin{bmatrix} A & B \\ C & D \end{bmatrix} \begin{bmatrix} V_1 \\ V_2 \end{bmatrix} \tag{6}$$

and

$$\beta_m = k\left(\nu^2 + H + K\right)^{1/2} \tag{7a}$$

$$W_m = \frac{W}{(\nu^2 + H + K)^{1/2}} \tag{7b}$$

$$\beta_s = k\left(\nu^2 + K\right)^{1/2} \tag{7c}$$

$$W_s = \frac{W_0}{(\nu^2 + K)^{1/2}} \tag{7d}$$

$$W_0 = \left(\frac{\mu_0}{\varepsilon_0}\right)^{1/2} = 120\pi. \tag{7e}$$

The image transfer constant $\theta_i (= j\beta(m+s) = jk(m+s)$ in the photonic crystal terminology) and the image impedances (from left and from right) are given by

$$\cosh\frac{\theta}{2} = \sqrt{AD}$$
$$Z_{01} = \left(\frac{AB}{CD}\right)^{1/2},\ Z_{02} = \left(\frac{BD}{AC}\right)^{1/2} \tag{8}$$

where Z_{01} and Z_{02} represent E/H at 11 or 22 in the eigenstate, respectively.

Next, we proceed to draw the dispersion curves of the 2-D photonic crystal of Fig. 2(a) and (b). For simplicity, we assume $f(x) = g(y)$, $n_0 = H = 1$. There are two ways this can be done.

1) We assume an arbitrary value for k (the free-space wavenumber) and assume some separation constant K and obtain image transfer constants in the x system and the y system, respectively. By keeping k (or λ) constant and sweeping K, one obtains the equifrequency dispersion curve in the wavenumber space.
2) It is convenient to draw an $\omega - (\beta_x, \beta_y)$ diagram along some representative directions, such as ΓX, ΓM, etc. Let us explain how to draw the curve along ΓY, i.e., $\beta_x = 0$. Using (8), we rewrite $\beta_x = 0$ as $A_x = 0$ or $D_x = 0$ since we have $\sqrt{AD} = 0$. We explicitly write the subscript x to A and D to emphasize focus on the x system. It means, given some $\lambda = 2\pi/k$, we solve $A_x = 0$ or $D_x = 0$ for K. Once we have this K, we replace K by $-K$ and calculate $\theta_y = 2\cosh^{-1}\sqrt{A_y D_y}$ to obtain β_y using it. We follow similar steps for $\Gamma M, XM$, etc., to finish the dispersion curves of Fig. 5(a) in the primitive Brillouin zone. Note that there is no "full bandgap."

We recalculated these curves using a finite difference time domain (FDTD) simulation program. As expected, the results completely agreed with the analytical results.

B. Line-Defect Photonic Crystal Waveguide

Our mathematical tool (separation of variables) works for more complicated structures, such as waveguides and resonators. Since no closed-form solution for such systems has been known, our system can serve as reference systems. (Previous analytical investigation [3], [4] did not consider such modified structures.) Again for simplicity, we start from the structure we just treated in Section III-A. Let the central "air" portion be widened by $a/2$, as shown in Fig. 2(c). Note that the dielectric function $\epsilon(x, y)$ is the sum of a function of x and that of y. We are interested in the wave function of the form $X(x)Y(y)$. We need a solution decaying for $x \to \pm\infty$ and propagating in the y direction. The electrical model for x, bisected at $x = 0$, is shown in Fig. 4(b). In order to have an even symmetric guided mode, the bisected circuit seen at $x = 0$ should be open circuited; therefore, we have

$$W_s + j\left(\frac{BD}{AC}\right)^{1/2} \tan\beta_s \frac{a}{4} = 0. \tag{9}$$

Given λ and solving (9) for K, we obtain θ_y. The dispersion curve in Fig. 5(b) (indicated by the solid line) stands for the even

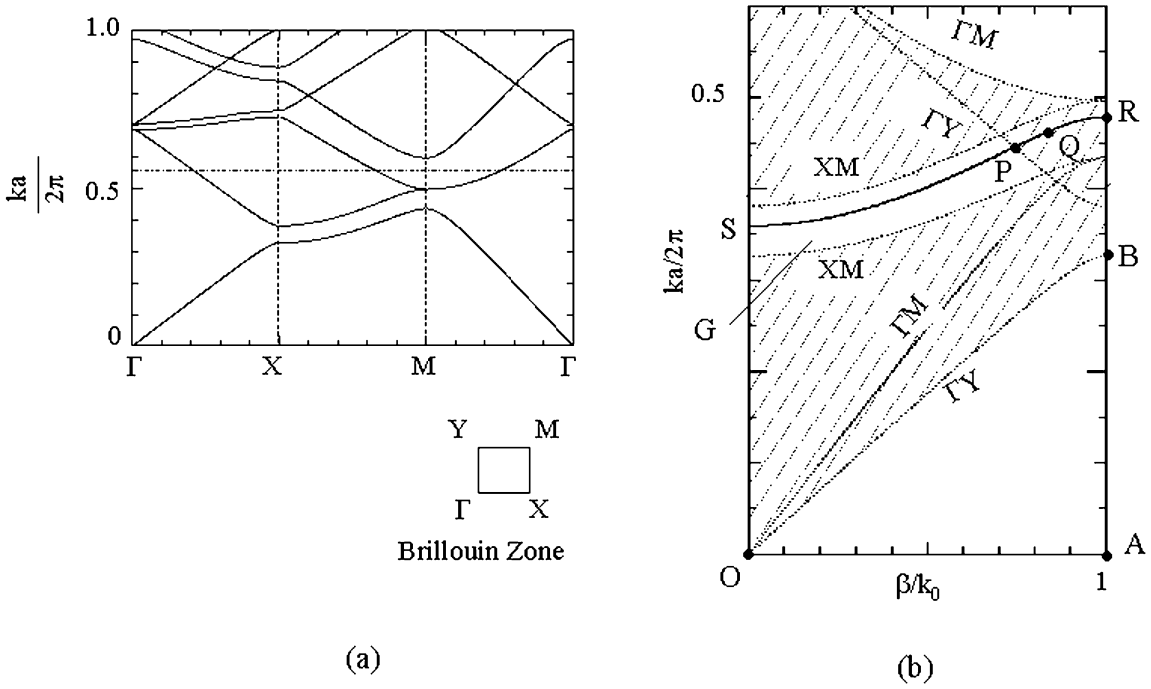

Fig. 5. (a) Band structure of a perfect crystal of Fig. 2(b). (b) Dispersion curve for the lowest guided mode (solid line) of a line-defect waveguide of Fig. 2(c).

guided mode. We find very interesting behavior of the mode along PQR [see Fig. 5(b)].

To help readers understand the situation, let us briefly summarize the situation of a "classical" dielectric waveguide where the cladding is uniform and a higher refractive-index core exists. In such structures, "continuum modes" fill the entire portion above the "clad line" roughly similar to OB [without a gap, such as the white stripe G above OB in Fig. 5(b)]. The guided modes form a finite number of curves lying in OAB. If one of the curves crosses the line OB, then it turns *leaky* beyond it.

Relating this to the crystal waveguide, note that the dispersion curve for the guided mode enters the "projection" of continuum modes [7]. In other words, the part PQR of the dispersion curve has the same wavenumber with a continuum mode (whereas the guided mode stays in the "bandgap region" when it is between P and S). One may be tempted to think our "guided" mode will couple to the continuum and therefore will leak along PQR. This guess is wrong, because this approach rigorously guarantees the existence of a lossless guided mode. The shape of equifrequency curves at point Q in the wavenumber space is shown in Fig. 6. The guided mode and the (degenerate) continuum mode are in different "branches": the guided mode lies in the stopband portion of branch A, while the radiation mode is in another branch B. The amplitude/intensity profiles are also shown. A computer simulation of this waveguide was done to confirm the propagating property [8]. As expected, the results agreed with our analysis.

Many groups work on photonic crystal waveguides, and their waveguides are more complicated; therefore, it is difficult to judge whether similar situations (degeneracy) exist. However, some experimental studies and simulation studies can be explained if there are leakage-free guided modes that degenerate with a continuum mode. For example, a recent study of a photonic crystal waveguide [4] reports that experiments and FDTD simulations indicate that there is a waveguiding effect beyond the "pure" guided wave region, where the guided modes do not overlap with any of continuum modes. This suggests the existence of a lossless (or at least low-loss leaky) guided mode beyond the "pure" region.

C. Crossed Line-Defect Resonator

Our technique of factorization also works for resonators. In the following, we present and solve a simple model. However, there will be a surprise—a completely localized mode exists in the absence of a complete bandgap in the host photonic crystal. The details follow.

The structure in Fig. 2(d) can localize a wave near the origin ($x = y = 0$): the factorization $Ez = X(x)Y(y)$ applies again. The same function works also in the y direction. We solved the resonance condition (assuming $X(x)$ and $Y(y)$ are identical) to obtain the resonance frequency $ka/2\pi = 0.5524$, and the field pattern for $X(x)$ [or $Y(y)$] is shown in Fig. 7. For the reader's convenience, the resonant frequency is shown by the horizontal dotted line ($ka/2\pi \sim 0.56$) in Fig. 5(a). The important point is that the mechanism of wave localization does not rely on the full-bandgap characteristics of the host photonic crystal. In fact, Fig. 5(a) shows the nonoverlapping property of bandgaps for different directions, so "classically" we do not expect wave localization.

Using Fig. 7, we can clearly explain why, in the absence of a full bandgap, we still have a lossless ($Q = \infty$) resonance mode not coupling with radiation. At the resonance, the equiintensity contour of the mode envelope forms straight lines with the tilt $\pm 45^\circ$ with respect to the x and y axis. Because of exponential decay of the envelope with respect to $|x|$ and $|y|$ at the

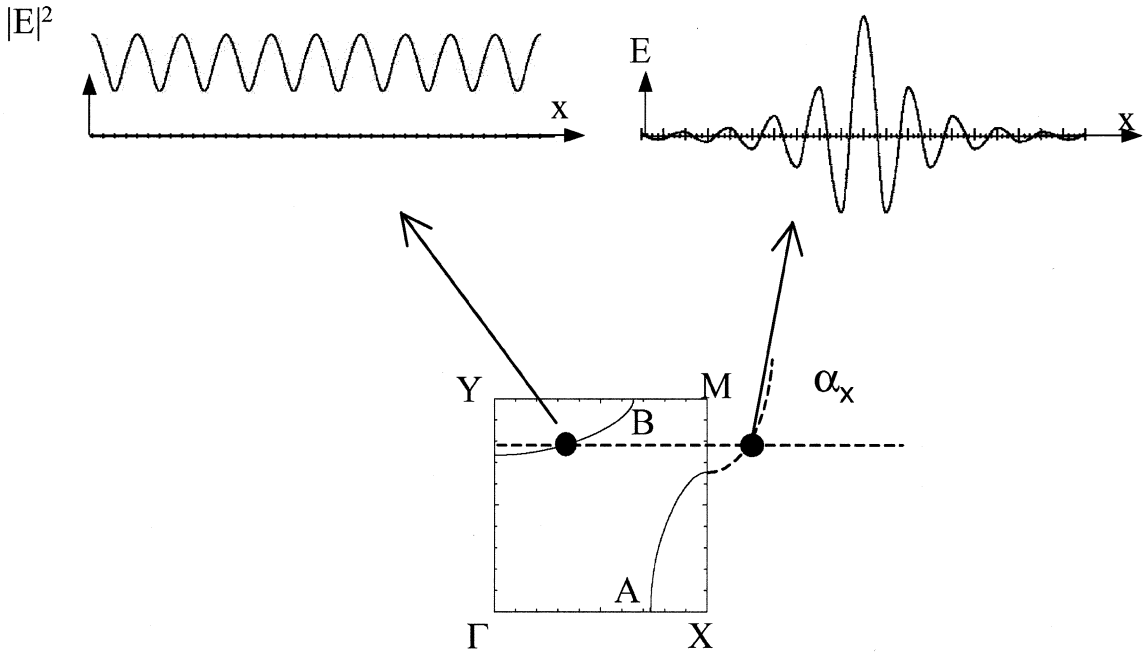

Fig. 6. Transverse field (or intensity) pattern of the guided mode and a continuum mode and their interpretation in the Brillouin zone.

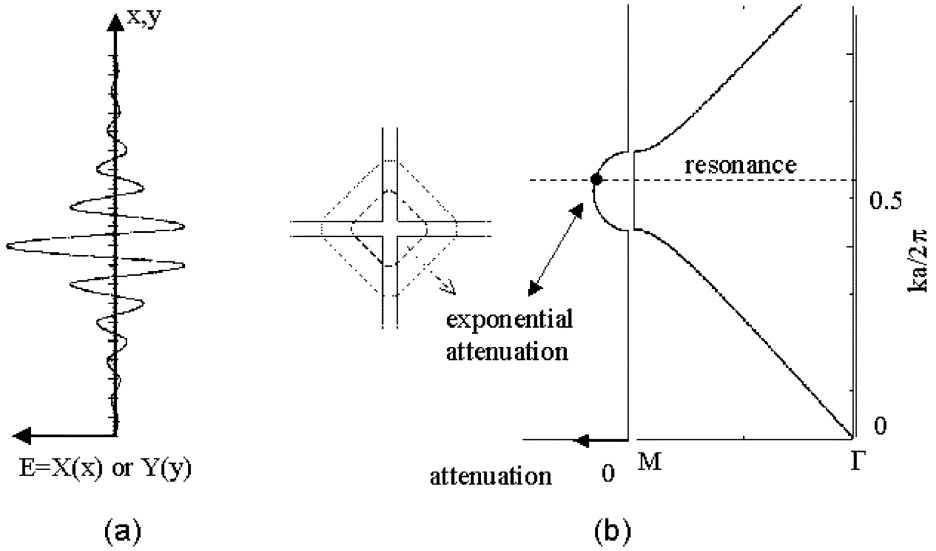

Fig. 7. (a) Resonant field factors $X(x)$ and $Y(y)$ for the lowest mode of the structure of Fig. 1(d). (b) The mechanism of wave trapping in the absence of a full bandgap.

same speed, the envelope has a factor such as $\exp[-\alpha(x+y)]$. The line defects divide the entire space into four quadrants in each of which one single Bloch wave represents the field: The Bloch wave is represented by a complex point near the point M in the Brillouin zone as shown in Fig. 7(b). The phase shift is the same as M, but small attenuation exists in the direction of M. (This resonance is different from the model of Sakoda [10], which considers uniform 2-D photonic crystal slabs and derives a lossless resonance where the field extends to infinity in the 2-D plane.)

Once again, this analysis was compared with a computer simulation [8]. The results (resonance frequency and the modal field) agreed again.

IV. Comments

The structures discussed thus far are infinitely long in the z direction and difficult to realize. They also require three kinds of dielectric materials and are inconvenient to fabricate as compared with usual two-material systems. We are curious whether similar "myth-breaking" effects take place in more "realistic" structures. The first question is, Can we avoid using infinitely long pillars? The answer is (practically) yes: we can localize waves near the plane $z = 0$ by increasing the dielectric constant of pillars near $z = 0$ [as discussed in [11], Fig. 1(a)], at the expense of slightly impairing the TE nature of waves. The second question is, Can we expect similar effects in a two-mate-

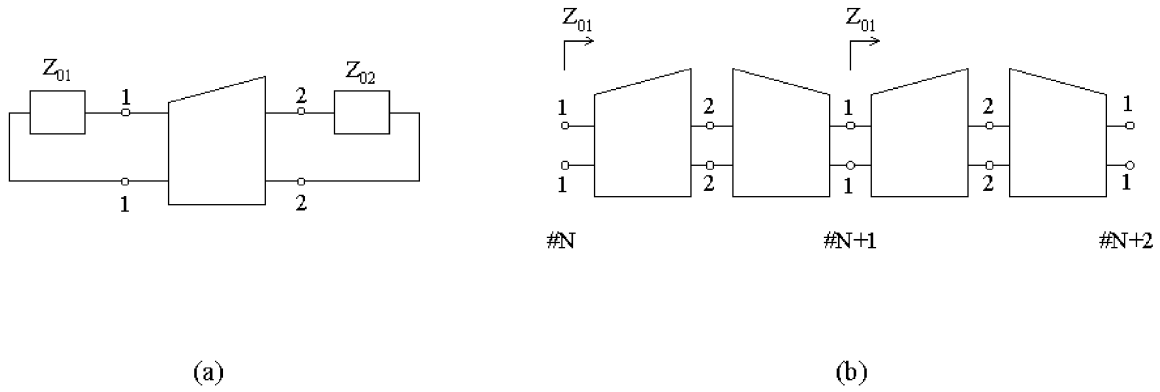

Fig. 8. (a) The smallest unit. (b) The whole chain of cascaded nonsymmetric circuits.

rial system? At present, we collaborate with simulation workers and have had positive results, which will be published in the near future. Furthermore, our principle can and is planned to be tested in microwave planar circuit models.

V. Conclusion

We proposed a new group of analytically solvable photonic crystal-related structures. Since such structures can be rigorously analyzed, they can serve as a reference crystal, waveguide, or resonator. They show some unexpected properties: existence of a nonleaky guided mode having an identical axial wavenumber with that of radiation modes and existence of a lossless resonance in the absence of a full bandgap. These facts add some new dimension to the existing theory of photonic crystal waveguides and resonators. We have to examine some of the common beliefs about photonic crystals more carefully.

Appendix

Basic Properties of Image Parameters

The method of image parameters [5] is ideally suited for the analysis of infinitely cascaded identical two-terminal-pair networks. Roughly speaking, the "image impedance" tells the eigenexcitation at the terminal pair, and the "image transfer constant" gives the phase shift (or decay of the amplitude) between excitations at neighboring terminal pairs.

Consider a circuit shown in Fig. 8(a). Assume that the input impedance seen from 11 is Z_{01} when 22 is terminated by Z_{02}; likewise, the impedance seen from 22 is Z_{02} when 11 is terminated by Z_{01}.

After a few calculations, we have

$$Z_{01} = \sqrt{\frac{AB}{CD}}, \qquad Z_{02} = \sqrt{\frac{BD}{AC}} \tag{A1}$$

where the $ABCD$ matrix is defined by

$$\begin{bmatrix} V_1 \\ I_1 \end{bmatrix} = \begin{bmatrix} A & B \\ C & D \end{bmatrix} \begin{bmatrix} V_2 \\ I_2 \end{bmatrix}. \tag{A2}$$

When one considers an infinite chain of circuits shown in Fig. 8(b) and assumes an eigen Bloch state (i.e., only the Bloch wave propagating to the right exists), the voltage to current ratio at 11 is Z_{01} while that at 22 is Z_{02}.

The image transfer constant between 11 and 22, defined by $\theta' = (1/2)\log(V_1 I_1 / V_2 I_2)$, is given by

$$\cosh\theta' = \sqrt{AD}. \tag{A3}$$

A and D are real numbers, and B and C are pure imaginary numbers. When Z_{01} and Z_{02} are positive real numbers, the circuit is in the passband and the eigen phase shift is real. When they are imaginary, the circuit is in the stopband and the eigen phase shift turns imaginary, which means a real eigen attenuation.

Thus far we have focused on the smallest unit, 11–22, in Fig. 8(b). When we consider "one full period," e.g., 11–22–11, its image transfer constant θ is given by $2\theta'$. Then θ simplifies to

$$\begin{aligned} \theta &= \log\frac{V_N}{V_{N+1}} = \frac{\log V_{N+1}}{V_{N+2}} = \cdots \\ &= \frac{\log I_N}{I_{N+1}} = \frac{\log I_{N+1}}{I_{N+2}} = \cdots \end{aligned} \tag{A4}$$

[see Fig. 8(b)].

Acknowledgment

The author expresses his gratitude to Dr. P. J. Roberts and T. Shepherd for information about [3], [4]. He sincerely thanks Dr. T. Kawashima for much discussion and carrying out calculations.

References

[1] E. Yablonovitch, "Photonic band-gap structure," *J. Opt. Soc. Amer. B, Opt. Phys.*, vol. 10, pp. 283–295, 1993.
[2] A. Mekis, J. C. Chen, I. Kurland, S. Fan, P. R. Villeneuve, and J. D. Joannopoulos, "High transmission through sharp bends in photonic crystal waveguide," *Phys. Rev. Lett.*, vol. 77, pp. 3787–3790, 1996.
[3] T. J. Shepherd and P. J. Roberts, "Scattering in a two-dimensional photonic crystal: An analytical model," *Phys. Rev. E, Stat. Phys. Plasmas Fluids Relat. Interdiscip. Top.*, vol. 51, pp. 5158–5161, 1995.
[4] W. Axmann, P. Kuchment, and L. Kunyansky, "Asymptotic methods for thin high-contrast two-dimensional PBG materials," *J. Lightwave Technol.*, vol. 17, pp. 1996–2007, Nov. 1999.
[5] E. A. Guillemin, *Synthesis of Passive Networks*. New York: Wiley, 1957, pp. 186–191.

[6] J. C. Slater, *Microwave Electronics*. New York: Van Nostrand, 1950, pp. 30–35.
[7] J. D. Joannopoulos, R. D. Meade, and J. N. Winn, *Photonic Crystals—Molding the Flow of Light*. Princeton, NJ: Princeton Univ. Press, 1995, pp. 94–104.
[8] S. Kawakami, T. Kawashima, M. Koshiba, and T. Watanabe, presented at the Meeting of the IEICE, Tokyo, Japan, Mar. 27, 2002, SC-1-5.
[9] E. Chow, S. Y. Lin, J. R. Wendt, S. G. Johnson, and J. D. Joannopoulos, "Quantitative analysis of bending efficiency in photonic-crystal waveguide bends at $\lambda = 1.55$ μm wavelength," *Opt. Lett.*, vol. 26, pp. 286–288, 2001.
[10] K. Sakoda and T. Ochiai, presented at the Ministry of Culture, Education, Sports, Science, and Technology's 5th Symp. Photonic Crystals, Tokyo, Japan, Feb. 2001.
[11] H. Benisty, D. Labilloy, C. Weisbuch, C. J. M. Smith, T. F. Krauss, D. Cassagne, A. Beraud, and C. Jouanin, "Radiation losses of waveguide-based two-dimensional photonic crystals: Positive role of the substrate," *Appl. Phys. Lett.*, vol. 76, pp. 532–534, 2000.

Shojiro Kawakami (S'60–M'65–SM'85–F'90–LF'02) received the Ph.D. degree in 1965 from the University of Tokyo, Japan.

He joined Tohoku University, Sendai, Japan, and, in 1979, became Professor. From the late 1960s through the 1970s, he was interested in optical fiber theory. He studied near square-law fibers and discovered its group-velocity equalization effect in 1967. He was then interested in single-mode fibers and, from 1974 to 1976, invented and analyzed W fibers, also called depressed clad fibers. In the 1980s, he started experimental works and invented several microoptic components, such as the laminated polarizer (LAMIPOL) and thermally diffused expanded core (TEC) fibers. In 1996, he found the principle of "autocloning" and started researching photonic crystals. Since 1999, he has been the leader of a national research project on photonic crytals from MEXT. He retired from Tohoku University and became Professor Emeritus in Spring 2000. He then moved to the New Industry Creation Hatchery Center (NICHe), Tohoku University, as Professor, where he is the leader of the Photonics Industry Creation Group and also the MEXT project. He is also the Founder of Photonic Lattice Inc., which started this past July.